Clim. Past Discuss., 8, 3831–3869, 2012
www.clim-past-discuss.net/8/3831/2012/
doi:10.5194/cpd-8-3831-2012

Climate of the Past Discussions

Climatic impacts of fresh water hosing under Last Glacial Maximum conditions: a multi-model study

M. Kageyama[1], U. Merkel[2], B. Otto-Bliesner[3], M. Prange[2], A. Abe-Ouchi[4], G. Lohmann[5], D. M. Roche[1], J. Singarayer[6], D. Swingedouw[1], and X. Zhang[5]

[1]LSCE/IPSL Laboratoire des Sciences du Climat et de l'Environnement, CEA-CNRS-UVSQ – UMR8212, CE Saclay, L'Orme des Merisiers, Bat. 701, 91191 Gif-sur-Yvette Cedex, France
[2]MARUM – Center for Marine Environmental Sciences, University of Bremen, Klagenfurter Strasse, 28334 Bremen, Germany
[3]NCAR, National Center for Atmospheric Research, 1850 Table Mesa Drive, Boulder, 80305, Colorado, USA
[4]AORI, Atmosphere and Ocean Research Institute, University of Tokyo, 5-1-5 Kashiwanoha, Kashiwa, 277-8568, Chiba, Japan
[5]Alfred Wegener Institute for Polar and Marine Research, Bussestr. 24, 27570 Bremerhaven, Germany
[6]Department of Geographical Sciences, University of Bristol, University Road Bristol, Bristol, BS8 1SS, UK

Received: 31 July 2012 – Accepted: 8 August 2012 – Published: 20 August 2012

Correspondence to: M. Kageyama (masa.kageyama@lsce.ipsl.fr)

Published by Copernicus Publications on behalf of the European Geosciences Union.

Abstract

Fresh water hosing simulations, in which a fresh water flux is imposed in the North Atlantic to force fluctuations of the Atlantic Meridional Overturning Circulation, have been routinely performed, first to study the climatic signature of different states of this circulation, then, under present or future conditions, to investigate the potential impact of a partial melting of the Greenland ice sheet. The most compelling examples of climatic changes potentially related to AMOC abrupt variations, however, are found in high resolution palaeo-records from around the globe for the last glacial period. To study those more specifically, more and more fresh water hosing experiments have been performed under glacial conditions in the recent years. Here we compare an ensemble constituted by 11 such simulations run with 6 different climate models. All simulations follow a slightly different design but are sufficiently close in their design to be compared. All study the impact of a fresh water hosing imposed in the extra-tropical North Atlantic. Common features in the model responses to hosing are the cooling over the North Atlantic, extending along the sub-tropical gyre in the tropical North Atlantic, the southward shift of the Atlantic ITCZ and the weakening of the African and Indian monsoons. On the other hand, the expression of the bipolar see-saw, i.e. warming in the Southern Hemisphere, differs from model to model, with some restricting it to the South Atlantic and specific regions of the Southern Ocean while others simulate a wide spread Southern Ocean warming. The relationships between the features common to most models, i.e. climate changes over the North and tropical Atlantic, African and Asian monsoon regions, are further quantified. These suggest a tight correlation between the temperature and precipitation changes over the extra-tropical North Atlantic, but different pathways for the teleconnections between the AMOC/North Atlantic region and the African and Indian monsoon regions.

CPD
8, 3831–3869, 2012

1 Introduction

Since their discovery in the North Atlantic marine sediment records and in the Greenland ice cores (Heinrich, 1988; Dansgaard et al., 1993), the abrupt events of the last glacial have been the topic of active research. On the palaeodata side, they were soon discovered to be of global extent (cf. the compilation by Voelker, 2002, and the more recent review by Clement and Peterson, 2008), with signatures in the tropical hydrological cycle (e.g. Peterson et al., 2000; Wang et al., 2004 for the Western Tropical Atlantic, Wang et al., 2001 for the East Asian monsoon) as well as the Antarctic temperatures (e.g. EPICA community members, 2006). In particular, Antarctic temperature changes were shown to have a specific timing with respect to Greenland abrupt temperature changes, with warmings (respectively cooling) in Antarctica when Greenland is in a cool (respectively warm) state (Blunier and Brook, 2001, confirmed by further works such as EPICA community members, 2006). This global expression of the glacial abrupt events and the fact that the global ocean circulation was known to theoretically have multiple equilibria (Stommel, 1961) pointed to the deep ocean circulation playing a major role in these events. The relative timings of Greenland vs. Antarctic temperature changes further confirmed this hypothesis which was formalised in the "bipolar see-saw" concept (Crowley, 1992; Stocker and Johnsen, 2003).

Fresh water hosing experiments, in which the Atlantic Meridional Overturning Circulation (AMOC) is perturbed by imposing a fresh water flux, usually in the North Atlantic, are useful numerical experiments to understand the mechanisms of climate change related to changes in AMOC. Such simulations have first been performed (e.g. Manabe and Stouffer, 1988) in the present or pre-industrial contexts to highlight the climate signature of different climate states. They are also motivated by the fact that most models appear to simulate a decrease in AMOC strength under increased atmospheric CO_2 concentrations (Gregory et al., 2005) and by the fact that the Greenland ice sheet could melt significantly in the future (Swingedouw et al., 2006). Stouffer et al. (2006) have compared the response of 9 Atmosphere-Ocean coupled General

CPD
8, 3831–3869, 2012

Circulation Models (AOGCMs) and 5 Earth System Models of Intermediate Complexity (EMICs, cf. Claussen et al., 2002, for a definition of EMICs) to fresh water hosings of 0.1 and 1 Sv imposed for 100 yr in the 50–70° N band of the North Atlantic. For the 0.1 Sv experiment, they find that no model simulates an AMOC collapse, the AMOC decrease ranging from 10 to 60 %. Common climatic responses in these simulations include North Atlantic cooling and a tendency for a southward shift of the Atlantic ITCZ. Some models simulate a northward shift of the Nordic Seas convection sites, which coincides with a warming to the north of the hosing area. The AMOC totally collapses in all models for a 1 Sv hosing, which is associated with larger surface climate response, in particular in terms of the southward shift of the ITCZ. Stouffer et al. (2006) highlight the common features of these hosing experiments but note that the models' sensitivities to hosing, mostly evident from the 0.1 Sv hosing experiment, are different and that their climatic response can also be different in some regions such as the high-latude Nordic Seas and the Arctic (in particular the Barents Sea).

However, the known abrupt events of the past have occurred in glacial conditions, which is a strong change in the boundary conditions compared to present ones. Using the CLIMBER-2 EMIC, Ganopolski and Rahmstorf (2001) showed that the glacial and pre-industrial states are characterised by different sensitivities to fresh water hosing in the North Atlantic, with a much narrower hysteresis of the AMOC as a function of the imposed fresh water flux in the glacial state. This result was later corroborated employing a three-dimensional ocean general circulation model (Prange et al., 2002) and could explain the high sensitivity of the AMOC, and therefore climate, under glacial conditions and therefore the occurrence of abrupt events preferentially in these glacial conditions. In a recent review on the climatic impacts of changes in AMOC, Kageyama et al. (2010) further showed the differences between performing hosing experiments under pre-industrial and glacial backgrounds by using two other EMICs, LOVECLIM and UVic. They highlighted the impact of the different sensitivities of these models to hosing, with in particular, an advection of the North Atlantic cooling signal to the Southern Ocean if the AMOC does remain active. Finally, they showed the differences between transient results and equilibrium results for the UVic models, some patterns of surface climate change, especially in the Southern Hemisphere, appearing very late in a hosing experiment.

The precise climatic response to the details of the hosing scenario has been studied with the LOVECLIM EMIC by Roche et al. (2010). They test different hosing amplitudes for 10 different regions and find significant differences in the responses for Arctic vs. Nordic Seas hosing. This could allow building climatic fingerprints characteristic of hosing in these regions and help constrain the hosing scenario for a given event. On the other hand Otto-Bliesner and Brady (2010) find no large difference in the climatic response between the two hosing regions they test, i.e. the Northern North Atlantic between 50 and 70° N and the Gulf of Mexico. They underscore that under AMOC resumption, the ITCZ recovers much faster than the AMOC, northern sea-ice and Greenland temperatures and simultaneously with tropical temperatures. The relationship between climatic changes in the North Atlantic and those in the tropical areas will be investigated here from multiple model output.

Indeed, one particularly intriguing and challenging aspect of the palaeodata from these times of abrupt changes is the remote teleconnections they suggest. Climatic changes in Europe, as characterised by pollen (Sánchez-Goñi et al., 2002) and speleothem (Genty et al., 2003) records have been connected to the Greenland climate changes, but further away, the ITCZ changes over the Western Tropical Atlantic (Cariaco Basin record, Peterson et al., 2000, vs. North East Brazil speleothem record, Wang et al., 2004), the dust record from the tropical East Atlantic (Jullien et al., 2007) and monsoon variations over China (e.g. the Hulu cave speleothem record of Wang et al., 2001), India (Leuschner and Sirocko, 2000) and Africa (Mulitza et al., 2008; Niedermeyer et al., 2009) have been correlated to the abrupt events recorded in Greenland and/or the North Atlantic. Clement and Peterson (2008) provide an extensive review on the mechanisms for these teleconnections related to AMOC variations, based on the hosing experiments published at that time, i.e. mainly under present day conditions. They classify the simulated responses to fresh water hosing in three categories:

CPD
8, 3831–3869, 2012

1. Those showing symmetric adjustments in the northern extratropics by advection of the North Atlantic cooling by the mean westerlies, this cooling then propagating to the tropics through the wind-evaporation-SST feedback (Chiang et al., 2008) in all basins. This then acts to shift the ITCZ southward in all basins as well.
2. Those simulating major changes in the North Atlantic, those changes propagating to the tropical areas in the Atlantic by atmospheric and ocean processes. These changes in the tropical Atlantic then trigger contrasted responses in the other tropical basins by modifications of the Walker cells. The global response is zonally asymmetric.
3. Those simulating fast oceanic teleconnections, related to wave propagation due to the sea-level height difference associated with the imposed fresh water flux in the North Atlantic.

From this review, we will retain the zonally symmetric or asymmetric character of the response of models for fresh water hosing. Such a differentiation has also been highlighted by Dima and Lohmann (2010) for the recent evolution of the AMOC and climate.

Since the reviews by Clement and Peterson (2008) and Kageyama et al. (2010), many hosing experiments have been produced using glacial boundary conditions. Some of these have been published (Kageyama et al., 2009; Swingedouw et al., 2009; Otto-Bliesner and Brady, 2010; Merkel et al., 2010; Roche et al., 2010; Singarayer and Valdes, 2010), others are in the process of being published (Zhang et al., 2012). Our aim here is to take the opportunity offered by the availability of these results and compare them. As shown by the topics of each of these publications, the objectives of each of these experiments were different, ranging from the sensitivity to hosing in different regions or to different hosing amplitudes (Roche et al., 2010; Otto-Bliesner and Brady, 2010) to the analysis of the impact of fresh water hosing on ENSO and its associated teleconnections (Merkel et al., 2010) or the impact of AMOC collapse under a wide set of boundary conditions (Swingedouw et al., 2009; Singarayer and Valdes, 2010). It is therefore an ensemble which was not initially devised for a clean model intercomparison but this ensemble gives a unique opportunity to compare model results for the glacial, as was done by Stouffer et al. (2006) for present conditions, albeit with a non pre-determined fresh water hosing set-up. This set-up and the AMOC response to the hosing are described in Sects. 2 and 3, respectively.

In comparing these simulations, we will first characterise regions of agreement/disagreement between the climate responses in surface air temperature and precipitation to fresh water hosing by considering both the amplitude and the sign of the response (Sect. 4). We then attempt, for those regions with consistent responses across models, to quantify the relationships between the responses in temperature and precipitation over a given region, or between climate changes of different regions (Sect. 5) and to see if they are consistent with those found in previous works. In particular, we investigate the climatic changes over the North Atlantic, the tropical Atlantic, the African and Indian monsoon regions. Section 6 summarizes our main findings and presents some perspectives to this first analysis.

2 Description of the numerical simulations

The comparison presented here is based on simulations that have been produced independently by 6 different palaeoclimate modelling groups, using 6 climate models, one of which (LOVECLIM) is a (rather complex) Earth System Model of Intermediate Complexity . A summary of the model characteristics and reference is provided in Table 1. The "MIROC1" and "MIROC2" experiments have been run using slightly different versions of the MIROC model, which yield similar pre-industrial climates but quite different LGM climates, in particular regarding the AMOC, which is strong (19 Sv) in the "MIROC1" version and weak (8.4 Sv) in the "MIROC2" version. The "COSMOS-S" and "COSMOS-W" LGM reference simulations have been produced with the same version of the COSMOS model but starting from different initial states, yielding very strong (26.8 Sv) and weaker (18.8 Sv) AMOCs (Zhang et al., 2012). The "CCSM-NCAR" and

CPD
8, 3831–3869, 2012

“CCSM-MARUM” experiments use the same model (CCSM3) but with different resolutions.

In total, we have analysed 11 sets of reference states/hosing experiments run with these 6 models. This is an “ensemble of opportunity” gathered from published (or existing but not yet published) simulations. There was no common protocol decided in advance by all the groups but we have endeavoured to gather experiments which were as close to each other as possible. Most groups have used the Last Glacial Maximum PMIP2 protocol (Braconnot et al., 2007, http://pmip2.lsce.ipsl.fr) for their reference simulation. The HadCM3 experiments use the slightly different state of 24 kyr BP. In terms of the ice-sheets, atmospheric greenhouse gases or orbital parameters, this state only slightly differs from the 21 kyr BP LGM state.

The “hosing” was applied as a fresh water flux over a large region of the North Atlantic (50–70° N, “Ruddiman belt” or Greenland-Iceland-Norwegian Seas, cf. Table 2 for details) and not at the outlet of the Saint Lawrence River or in the Gulf of Mexico. In none of the experiments this fresh water hosing was compensated elsewhere on the globe. Its value ranges from 0.1 to 0.4 Sv. The rationale behind this range was to use “realistic” values of hosing (compared to the other often used value of 1 Sv, cf. Roche et al., 2004) but also to obtain states with weak AMOC and significant climatic responses even for models which proved not to be very sensitive to fresh water hosing: LOVECLIM and HadCM3 have a rather small response to fresh water hosing values of 0.15 and 0.1 Sv respectively, so for these models we have included hosing simulations with stronger fresh water hosing values, which result in a stronger response in AMOC and climate, in our comparison.

The simulations had different durations and at times, the full time series of the experiment was not available for analysis for technical reasons. This is why we could not analyse simulations for the same period after start of hosing. Most simulations were at equilibrium for the reference climate but not necessarily for the perturbed AMOC state, in particular in terms of Southern Ocean or deep ocean temperatures. The results shown here should therefore be viewed as transient responses to the corresponding

CPD
8, 3831–3869, 2012

fresh water perturbations. This is why we only rapidly document the AMOC response in the next section and we have focused most of our analysis on the surface climatic response, attempting to characterise the relationship between different aspects of surface climate in one region (e.g. temperature vs. precipitation) and on the relationships between climate responses in different regions of the globe for which fast teleconnections mechanisms have been suggested by previous work, as briefly summarised in the introduction.

3 Response of the Atlantic Meridional Overturning Circulation

Figure 1 shows the response of the AMOC, defined as the (volume) export at 30° S in the Atlantic Ocean, to fresh water hosing. The top panels show this reponse in terms of the AMOC anomaly and relative anomaly as a function of the hosing applied. The range of results obtained for the 0.1 Sv hosing shows the diverse sensitivities of the models to fresh water hosing, with a nearly complete collapse for MIROC1, both COSMOS runs and IPSL. The CCSM AMOC anomalies do not appear as very large but the AMOC in the reference state for these models is rather small, so the relative decrease in AMOC for these models is quite large: 40 % for CCSM-NCAR, more than 60 % for CCSM-MARUM. As explained in the previous section, HadCM3 and LOVECLIM had the weakest sensitivities to fresh water hosing, which is shown by the less than 30 % decrease in AMOC for the hosing values of 0.1 Sv for HadCM3 and 0.15 Sv for LOVECLIM, so hosing experiments using stronger hosing values of 0.4 and 0.3 Sv were included in this comparison. These result in a decrease in AMOC close to 70 % for HadCM3 and to 80 % for LOVECLIM.

Figure 1c shows that the AMOC anomalies for the 0.1 Sv experiments appear to be linearly related to their refence value. This relationship does not hold when the additional experiments are included, or in terms of the relative AMOC change (Fig. 1d). Of course, the AMOC anomaly in response to hosing cannot be strong if the reference

CPD
8, 3831–3869, 2012

AMOC is weak (Fig. 1c). But collapse is obtained for reference states with strong (COSMOS) or quite weak (IPSL) AMOC (Fig. 1d).

In summary, we have a set of hosing experiments for full glacial states exhibiting a large range of AMOC responses to fresh water hosing. For the following analysis we retain that two hosing experiments still have an active AMOC, even if it is weaker than in the reference state. Those simulations are HadCM3-0.1 and LCM10-0.15, for which the perturbed AMOC is larger than 10 Sv. CCSM-NCAR's perturbed AMOC, equal to 9.3 Sv, is also close to this value. All other experiments exhibit a slow or nearly collapsed AMOC.

4 A global picture of the surface climate responses to fresh water hosing

4.1 Mean annual surface air temperature response

Figure 2 shows the response of each model to fresh water hosing in terms of mean annual surface air temperature. As expected from the experimental design, all models produce their strongest thermal response over the extra-tropical North Atlantic Ocean. Cooling is also found in the Nordic Seas and the Arctic in all models. This contrasts with the results shown for the present climate in the comparison by Stouffer et al. (2006), for which warming was obtained in some of the models north of the hosing region due to a northward shift of the deep convection sites and amplification of its impact by the sea-ice changes through modulation of surface albedo and atmosphere-ocean heat fluxes. For a glacial state, this phenomenon therefore does not seem to occur, which could be due to two factors: the deep convection sites are usually located more to the south and sea-ice is more extensive in LGM runs.

Although all models simulate a cooling over the North Atlantic extratropics, Nordic Seas and the Arctic Ocean in response to fresh water perturbation, the magnitude of this cooling varies widely from model to model, as shown by the standard deviation of the mean annual temperature response (Fig. 3, top). The North Atlantic and the southern part of the Nordic Seas show a larger range of model responses, with a standard deviation reaching more than 5 °C. This range in model responses can also be seen from the individual model results shown on Fig. 2, in which the response of MIROC2, with a cooling of around 2 °C, contrasts with the larger than 7.5 °C cooling simulated by e.g. CCSM-NCAR. Part of this large range in model response could be assigned to the range in AMOC responses to hosing, but another part could be attributed to the sea-ice extent in the reference state and the possible amplification of the hosing-induced cooling response by the sea-ice feedbacks. This amplification is strong in the CCSM-NCAR experiment, as explained by Otto-Bliesner and Brady (2010). It could be that the response of this model is rather strong because the reference LGM winter sea-ice over the Western North Atlantic is quite extensive for CCSM, as shown in comparison to other models by Kageyama et al. (2006) and Otto-Bliesner et al. (2007).

This cooling over the North Atlantic extratropics propagates along the Atlantic subtropical gyre, i. e. along the African west coast and then westward north of the equator. The extent of this propagation and the amplitude of the cooling signal are model dependent. Otto-Bliesner and Brady (2010) also point that for the CCSM-NCAR model they are fresh water flux dependent. Here, for instance, the cooling is very strong (up to 5 °C in amplitude) and extends all the way to tropical America in HadCM3-0.4 while it does propagate to tropical America but amounts to only 1 °C in CCSM-NCAR, despite the very strong cooling simulated by this model in the North Atlantic extra-tropics. Comparatively, the response of the MIROC2 model is nearly as strong over the tropics for a much weaker North Atlantic extratropical cooling.

Cooling is also consistently found by all models on at least some regions of Eurasia, as shown by the number of models simulating a temperature decrease larger than 0.5 °C (in amplitude) displayed on Fig. 3, bottom. The simulated cooling is usually not uniform over the whole Eurasian continent and this diagnostic shows that the number of models simulating a cooling over Eurasia is maximum over a region around 60° E. This corresponds to the fact that some models simulate less cooling, or, for HadCM3-0.1, even a small warming, over Europe and that the cooling does not extend to the same

CPD
8, 3831–3869, 2012

longitude for all models. This feature of decreased cooling over Europe was observed in the IPSL_CM4 simulation by Kageyama et al. (2009) and attributed to a southwesterly wind anomaly associated with the North Atlantic cooling. This behaviour could therefore be present in other models but unfortunately we did not have the necessary atmospheric circulation fields to check this in the framework of the present comparison.

Over the rest of the Northern Hemisphere, and especially over the northeast Pacific and North America, no consistent cooling is simulated. This shows the limits of transport of the cool anomaly by simple advection, but also, as for Europe, potential impacts of atmospheric circulation changes which we leave for further investigation.

Over the Southern Hemisphere, as seen in the introduction, the expected response, at least for simulations in which the AMOC strongly decreases, is a warming of the South Atlantic ocean and of the Southern Ocean, i.e. the expression of the bi-polar see-saw. Figures 2 and 3 show that this response is not as consistently simulated as the North Atlantic cooling. A majority of models do simulate a warming over the South Atlantic Ocean and some regions of the Southern Ocean, over the Indian Ocean sector, south of Australia and over the Southwest Pacific but only a minority of models simulate a warming over the Southeast Pacific. This is not surprising in experiments such as LCM10-0.15 or HadCM3-0.1, which retain an active AMOC. These are then able to transport the North Atlantic cooling anomaly to the Southern Hemisphere via this remaining global overturning circulation. In simulations in which the AMOC strongly collapses, we can distinguish between models showing a warming on all longitudes of the Southern Ocean (e.g. CCSM-NCAR, MIROC1) and others which display zonally asymmetric patterns, such as LCM10-0.30 or IPSL. The fact that warming is not consistently found for all longitudes of the Southern Ocean might be due to the available experiments being far from the equilibrium response and the warming associated with the bipolar see-saw needing time to propagate throughout the Southern Ocean. There could also be faster mechanisms which could prevent the establishment of a zonally homogeneous Southern Ocean warming. Buiron et al. (2012) suggest such a mechanism to be active in the IPSL_CM4 experiment, where cooling in the Southeast Pacific is happening on timescales of a few decades as a result of a coupled atmosphere-surface ocean teleconnection with the tropical Atlantic. The southward shift of ITCZ (cf. next section) over the tropical Atlantic appears to trigger this teleconnection.

In summary, as expected from the experimental design of the hosing simulations, the most consistent surface air temperature response across the models is the North Atlantic cooling, extending over much of extra-tropical Eurasia. The intensity of this cooling ranges from a couple of °C to more than 7.5 °C. The eastward extension over Eurasia and, downstream, over the Pacific, are very model-dependent and almost no model simulates a cooling over North America. However, we can distinguish experiments whose response in the northern extra-tropics is nearly zonal (CCSM-NCAR, CCSM-MARUM, MIROC1) from simulations in which it is clearly zonally asymmetric (IPSL, LCM10-0.15, LCM10-0.30). The "zonally symmetric" models are also those for which the warming is most extensive and strongest over the Southern Ocean. For this region, there is less consistency, even in sign, of the model responses to hosing in the North Atlantic. Zonal aysmmetries and for some models cooling in some regions of the Southern Ocean, are inconsistent with the traditional view of the bi-polar see-saw. This could only be a transient response or the result of faster, atmosphere-surface ocean, teleconnections from the Tropics. To distinguish between those, we would need much longer experiments which were not available for all models for this comparison exercise.

4.2 Mean annual precipitation response

The precipitation response to hosing is shown on Figs. 4 and 5 for the same years as for the temperature response discussed in the previous section. Consistently with the temperature decrease over the North Atlantic, the precipitation decreases there for all models. This is consistent with the Clausius-Clapeyron relationship, but also with the fact that a more extensive sea-ice cover prevents evaporation. In the next section, we will investigate if the magnitude of the decrease in precipitation relates to the amplitude of the cooling over this region.

CPD
8, 3831–3869, 2012

Nearly all models show an increase in precipitation over the tropical Atlantic south of the equator, while they show a decrease in precipitation just north of the equator and in the African monsoon region. Most models therefore simulate a southward shift of the Atlantic ITCZ, even those with modest AMOC weakening. The atmospheric component of LOVECLIM model being based on a quasi-geostrophic formulation, the tropical/equatorial atmospheric circulation is not very well represented in this model so the precipitation response is not very clear for the LCM10-0.15 simulation (weak AMOC decrease). It is nonetheless surprinsingly clear in the LCM10-0.30 run, with strong AMOC reduction, for which the precipitation response associated with the ITCZ southward shift and decrease in the African monsoon in the other models can be recognised for this EMIC too. The ITCZ southward shift extends to other tropical regions in some of the models, especially those which showed a strong extra-tropical temperature response outside the Atlantic region. The response over the tropical Pacific Ocean is, however, quite model dependent since the maps showing the number of models simulating an increase or decrease in precipitation (Fig. 5) do not show any consistent pattern there.

The Indian monsoon appears to weaken in most of the model experiments with a strong AMOC decrease, with the exception of the LOVECLIM model which is not well suited to resolve this particular feature. This consistent response is quite remarkable given the number of factors which can affect the Indian monsoon and given the fact that this climatic feature is of smaller scale compared to the other features discussed in this section.

In the following section, we investigate potential relationships between these changes in precipitation and the temperature changes described in Sect. 4.1.

Discussion Paper | Discussion Paper | Discussion Paper | Discussion Paper |

CPD
8, 3831–3869, 2012

Climatic impacts of FW hosing for LGM conditions

M. Kageyama et al.

5 An attempt at quantifying the relationships between the responses of AMOC, temperature and precipitation, to fresh water hosing

Here we study the relationshipd between AMOC changes and averages of the temperature and precipitation anomalies over key regions, defined as follows:

- the "North Atlantic" (extra-tropical North Atlantic): 50–10° W, 40–60° N;
- the "North Tropical Atlantic": 50–15° W, 5–30° N;
- the "North Equatorial Atlantic": 50–15° W, 5–15° N;
- the "South Tropical Atlantic": 30° W–10° E, 20° S–5° N;
- the "African monsoon region": 15° W–15° E, 5–15° N;
- the "Indian monsoon region": 60–90° E, 10–30° N;
- the "Indian Ocean": 50–100° E, 10° S–15° N.

5.1 The North Atlantic

As we have seen in Sect. 4.1, the most consistent impact of hosing, found in all models, is the cooling of the North Atlantic Ocean in the extra-tropics. Figure 6, top, shows that the amplitude of this cooling is only vaguely related to the AMOC decrease. This shows that other factors come into play to explain this amplitude: temperatures/presence of sea-ice in the reference state, large change in sea-ice cover between the hosing and the reference experiments are good candidates which unfortunately we could not test from the available data.

A much better relationship is found between temperature and precipitation changes (Fig. 6, bottom) over the North Atlantic region. If we except the result from the COSMOS-W experiment, the relationship is even nearly linear, with precipitation changes ranging from nearly zero to $-1\,\mathrm{mm\,day^{-1}}$ for temperature changes ranging from −1 to −14 °C. The COSMOS-W relatively weak decrease in precipitation compared to its strong cooling can be explained by the fact that in the southern part of the region on which the "North Atlantic" average is computed, precipitation is actually simulated to increase (Fig. 4). This behaviour is also found for other models such as in experiments CCSM-NCAR, CCSM-MARUM and HadCM3-0.4 and is consistent with a southward shift of the Atlantic storm-track, which could be related to the southward displacement of the mid-latitude thermal front. The region of precipitation increase is however narrower in these other models than in COSMOS-W.

5.2 The Tropical Atlantic

Figure 7 investigates the relationships involving temperature changes over the Northern and Southern Tropical Atlantic. The top panels show that there is no systematic relationship between the AMOC changes and the temperature changes over these regions. Searching for stronger relationships, we then investigate if there is any with the North Atlantic extratropical temperature changes (the "North Atlantic" region defined in the same way as in Sect. 5.1 above). Figure 7c and d shows, again, little consistency between NorthTropicalAtlantic temperature cooling and NorthAtlantic cooling or between SouthTropicalAtlantic temperature cooling and NorthAtlantic cooling. The only feature that emerges from these figures is that no strong NorthTropicalAtlantic cooling is obtained for strong NorthAtlantic cooling while strong SouthTropicalAtlantic warming is only obtained for strong NorthAtlantic cooling. This explains that there is little consistency between North and South Tropical Atlantic temperature changes (Fig. 7e).

Figure 8 then investigates the changes in Tropical Atlantic precipitation. For the northern side of the equator, we have computed averages over a more restricted region than for the temperatures because precipitation changes were restricted to the southern part of the NorthTropicalAtlantic region defined in Fig. 7. This region defined to characterize precipitation changes north of the equator is labelled "NorthEqAtlantic". Figure 8c shows that precipitation changes on the northern and southern side of the equator are anti-correlated, with the strongest increase in precipitation south of the

Discussion Paper | Discussion Paper | Discussion Paper | Discussion Paper |

CPD

8, 3831–3869, 2012

Climatic impacts of FW hosing for LGM conditions

M. Kageyama et al.

equator occurring for models which also simulate the strongest decrease in precipitation north of the equator. Taken individually, precipitation changes over these regions correlate reasonably well with the underlying temperature changes (Fig. 8a and d). Given the absence of relationship between tropical temperature changes and North Atlantic temperature changes, it is not surprising to see no consistency between tropical precipitation changes and the North Atlantic extratropical temperature changes either.

In summary, the changes in tropical precipitation over the Northern and Southern Tropical Atlantic correlate well with the underlying temperature changes. The precipitation changes north and south of the equator are anti-correlated, confirming a relationship between those consisting in a southward shift of the ITCZ. These changes, however, do not appear to be strongly correlated to either the AMOC changes or the North Atlantic extratropical temperature changes, indicating that the extra-tropical – tropical connections are model dependent.

5.3 The African and Indian monsoons

The mean annual precipitation over the African monsoon region was shown to consistently decrease in most models (Fig. 5). Figure 9 attemps to quantify the relationships between the precipitation changes simulated over this region and surface temperature changes over the key regions investigated so far. This figure shows that it is actually very difficult to find a consistent relationship with temperature changes over any of these regions (NorthAtlantic, NorthTropicalAtlantic, NorthEqAtlantic and SouthTropicalAtlantic). The latter two regions appear to yield slightly better correlations than the former two. Precipitation changes over the African monsoon regions are therefore not following relationships as strong as for the nearby Atlantic ITCZ.

Further away from the Atlantic, the Indian monsoon region also showed a consistent decrease in precipitation among the models. Figure 10 shows that there is little correlation between these precipitation changes and the Indian Ocean temperature changes, nor with the NorthTropicalAtlantic changes. The correlation improves

Discussion Paper | Discussion Paper | Discussion Paper | Discussion Paper |

CPD

8, 3831–3869, 2012

Climatic impacts of FW hosing for LGM conditions

M. Kageyama et al.

for the NorthAtlantic extratropical temperature changes, albeit with a large dispersion for strong NorthAtlantic coolings. The best correlation is obtained with temperature changes over the SouthTropicalAtlantic region. The relationship could be non linear, with precipitation decrease over the Indian monsoon region getting stronger and stronger for stronger warming over the SouthTropicalAtlantic region, although admittedly this conclusion would be hard to sustain without the strong response of the HadCM3-0.4 model. These relationships suggest a tropical pathway in the response of the Indian monsoon to fresh water hosing. Marzin et al. (2012) actually find such a pathway by performing sensitivity experiments to the North Atlantic extratropical vs. Tropical Atlantic SST changes due to fresh water hosing with the IPSL model. They argue that the tropical SST changes are an efficient way of pulling the subtropical jet-stream southward over Africa and downstream, which results in a cooling of upper tropospheric temperatures over the Tibetan plateau and finally in a weakening of the Indian monsoon. It would be interesting, if we had the wind fields and the upper temperature fields for each model, to check if this mechanism occurs here, but at least the relationship between the SouthTropicalAtlantic temperatures changes and the changes over the Indian monsoon region are consistent with this explanation.

6 Conclusions

In this work, we performed a first comparison of fresh water hosing experiments run under full glacial conditions. We compared 6 models and 11 sets of simulations in total. These were not run with the specific objective of performing this comparison, which explains that we had a restricted list of common variables available for analysis.

The main conclusions from our comparison can be summarised as follow:

- The AMOC response to a 0.1 Sv fresh water flux imposed in the North Atlantic varies from a very small decrease to a near collapse. This range is much larger than the results for the pre-industrial comparison of Stouffer et al. (2006) but we have considered longer experiments here.

- The regions with consistent behaviour in their response to fresh water hosing are: the North Atlantic for temperatures and precipitation, the Tropical Atlantic, the regions of the African and Indian monsoon for precipitation. This is in line with palaeoclimatic evidence of abrupt events occurring during Heinrich events, as briefly reviewed in Sect. 1. We do not find a consistent response over South East Asia, in terms of precipitation. This could be due to the rather simplified experimental set-ups used here and in particular to our not using MIS 3 insolation, which would favour boreal summer insolation and therefore the Asian monsoons (Van Meerbeeck et al., 2009; Merkel et al., 2010; Kageyama et al., 2010). It could also be due to the Indian monsoon actually affecting the South East Asian monsoon records, as suggested from the modelling work of Pausata et al. (2011). Over these regions with consistent response, the amplitude of this response is, however, model dependent and more work is needed to finely compare model results to data, which would require more realistic boundary conditions. These results are qualitatively similar to those obtained for the pre-industrial background by Stouffer et al. (2006) with the exception of the behaviour over the Northern Nordic Seas and the Arctic for which no model simulates a warming for our glacial background state.

- Regions with inconsistent behaviour include the Northeast Pacific, the Southern Ocean and especially Southeast Pacific and Antarctica. Even though some data are available for Chilean coast and, of course, Antarctica, more data would help discriminating between models/hosing scenarios/mechanisms. A first distinction in the model responses are between those simulating a weak AMOC decrease and those simulating a strong AMOC decrease. The former ones appear to transport the northern cooling to the Southern Ocean. Only the latter ones simulate a bi-polar see-saw. This bi-polar see-saw can then take a zonally symmetric or a zonally asymmetric form, hence confirming the classification proposed by Clement and Peterson (2008). Indeed, those models who present a zonally symmetric response in the Southern Hemisphere generally also present a large

CPD
8, 3831–3869, 2012

cooling in the Northern Hemisphere extratropics. As far as this bi-polar see-saw is concerned, however, we must remain cautious in our comparison and conclusions since there could be differences in timing of the climatic response which we will have to investigate further.

- There is a linear relationship between local temperature and local precipitation changes over the North Atlantic and over the Tropical Atlantic, but no obvious relationship between North Atlantic temperature changes and AMOC changes, or between tropical Atlantic temperature/precipitation changes, and AMOC or North Atlantic temperatures. This suggests different extra-tropical-tropical teleconnection mechanisms in the different models.

- African monsoon consistently decreases for all models but it is difficult to relate the amount of precipitation decrease to temperature changes over the adjacent tropical Atlantic or to North Atlantic SST changes as suggested from the data presented by Niedermeyer et al. (2009): more analysis is required for this region at the seasonal level and it would be helpful to analyse atmospheric circulation changes in addition to the basic temperature and precipitation comparison presented here.

- The Indian monsoon weakening appears to be correlated both with North Atlantic and South Tropical Atlantic coolings. This suggests different teleconnection pathways for the different models. Here we would need specific sensitivity experiments to disentangle to response of the different models.

This comparison is therefore a first step in characterising and understanding the mechanisms at work in fresh water hosing experiments. It is based on an ensemble of rather idealised experiments given the fact that most abrupt events occurred during the different background climate of MIS 3. However, even though we do not fully understand them, the fact that we find results quite consistent with the previous comparison of Stouffer et al. (2006) performed for present boundary conditions, especially in terms

CPD
8, 3831–3869, 2012

of tropical response, is quite encouraging. We now need more specific sensitivity experiments to better understand each teleconnection, in the same way as has been performed for the present and for idealised geographical set-ups (cf. the review by Clement and Peterson, 2008).

The publication of this article is financed by CNRS-INSU.

References

Blunier, T. and Brook, E. J.: Timing of millenial-scale climate change in Antarctica and Greenland during the last glacial period, Science, 291, 109–112, 2001. 3834

Braconnot, P., Otto-Bliesner, B., Harrison, S., Joussaume, S., Peterchmitt, J.-Y., Abe-Ouchi, A., Crucifix, M., Driesschaert, E., Fichefet, Th., Hewitt, C. D., Kageyama, M., Kitoh, A., Laîné, A., Loutre, M.-F., Marti, O., Merkel, U., Ramstein, G., Valdes, P., Weber, S. L., Yu, Y., and Zhao, Y.: Results of PMIP2 coupled simulations of the Mid-Holocene and Last Glacial Maximum – Part 1: experiments and large-scale features, Clim. Past, 3, 261–277, doi:10.5194/cp-3-261-2007, 2007. 3839

Buiron, D., Stenni, B., Chappellaz, J., Landais, A., Baumgartner, M., Bonazza, M., Capron, E., Frezzotti, M., Kageyama, M., Lemieux-Dudon, B., Masson-Delmotte, V., Parrenin, F., Schilt, A., Selmo, E., Severi, M., Swingedouw, D., and Udisti, R.: Regional imprints of millennial variability during the MIS 3 period around Antarctica, Quaternary Sci. Rev., 48, 99–112, 2012. 3843

Chiang, J. C. H., Cheng, W., and Bitz, C. M.: Fast teleconnections to the Tropical Atlantic sector from Atlantic thermohaline adjustment, Geophys. Res. Lett., 35, L07704, doi:10.1029/2008GL033292, 2008. 3837

Claussen, M., Mysak, L., Weaver, A., Crucifix, M., Fichefet, T., Loutre, M.-F., Weber, S., Alcamo, J., Alexeev, V., Berger, A., Calov, R., Ganopolski, A.and Goosse, H., Lohmann, G., Lunkeit, F., Mokhov, I., Petoukhov, V., Stone, P., and Wang, Z.: Earth system models of intermediate complexity: closing the gap in the spectrum of climate system models, Clim. Dynam., 15, 579–586, 2002. 3835

Clement, A. C. and Peterson, L. C.: Mechanisms of abrupt climate change of the last glacial period, Rev. Geophys., 46, RG4002, doi:10.1029/2006RG000204, 2008. 3834, 3836, 3837, 3850, 3852

Collins, W. D., Blackmon, M., Bitz, C. M., Bonan, G. B., Bretherton, C. S., Carton, J. A., Chang, P., Doney, S. C., Hack, J. J., Kiehl, J. T., Henderson, T., Large, W. G., McKenna, D., Santer, B. D., and Smith, R.: The Community Climate System Model: CCSM3, J. Climate, 19, 2122–2143, 2006. 3858

Crowley, T. J.: North Atlantic deep water cools the Southern Hemisphere, Paleoceanography, 7, 489–497, 1992. 3834

Dansgaard, W., Johnsen, S. J., Clausen, H. B., Dahl-Jensen, D., Gundestrup, N. S., Hammer, C. U., Hvidberg, C. S., Steffensen, J. P., Sveinbjörnsdottir, A. E., Jouzel, J., and Bond, G.: Evidence for general instability of past climate from a 250-kyr ice-core record, Nature, 364, 218–220, 1993. 3834

Dima, M. and Lohmann, G.: Evidence for two distinct modes of large-scale ocean circulation changes over the last century, J. Climate, 23, 5–16, 2010. 3837

Driesschaert, E., Fichefet, T., Goosse, H., Huybrechts, P., Janssens, I., Mouchet, A., Munhoven, G., Brovkin, V., and Weber, S. L.: Modeling the influence of Greenland ice sheet melting on the Atlantic meridional overturning circulation during the next millennia, Geophys. Res. Lett., 34, L10707, doi:10.1029/2007GL029516, 2007. 3858

EPICA community members: One-to-one coupling of glacial climate variability in Greenland and Antarctica, Nature, 444, 195–198, doi:10.1038/nature05301, 2006. 3834

Ganopolski, A. and Rahmstorf, S.: Rapid changes of glacial climate simulated in a coupled climate model, Nature, 409, 153–158, 2001. 3835

Genty, D., Blamart, D., Ouahdi, R., Gilmour, M., Baker, A., Jouzel, J., and Van-Exter, S.: Precise dating of Dansgaard-Oeschger climate oscillations in Western Europe from stalagmite data, Nature, 421, 833–937, 2003. 3836

CPD
8, 3831–3869, 2012

Climatic impacts of FW hosing for LGM conditions

M. Kageyama et al.

Gordon, C., Cooper, C., Senior, C., Banks, H., Gregory, J., Johns, T., Mitchell, J., and Wood, R.: The simulation of SST, sea ice extents and ocean heat transports in a version of the Hadley Centre coupled model without flux adjustments, Clim. Dynam., 16, 147–168, 2000. 3858

Gregory, J. M., Dixon, K. W., Stouffer, R. J., Weaver, A. J., Driesschaert, E., Eby, M., Fichefet, T., Hasumi, H., Hu, A., Jungclaus, J. H., Kamenovitch, I. V., Levermann, A., Montoya, M., Murakami, S., Nawrath, S., Oka, A., Sokolov, A. P., and Thorpe, R. B.: A model intercomparison of changes in the Atlantic thermohaline circulation in response to increasing atmospheric CO_2 concentration, Geophys. Res. Lett., 32, L12703, doi:10.1029/2005GL023209, 2005. 3834

Heinrich, H.: Origin and consequences of cyclic ice rafting in the Northeast Atlantic ocean during the past 130 000 years, Quaternary Res., 29, 142–152, 1988. 3834

Jullien, E., Grousset, F., Malaize, B., Duprat, J., Sanchez-Goni, M. F., Eynaud, F., Charlier, K., Schneider, R., Bory, A., Bout, V., and Flores, J. A.: Low-latitude "dusty events" vs. high-latitude "icy Heinrich events", Quaternary Res., 68, 379–386, 2007. 3836

K-1 model developers: K-1 coupled model (MIROC) description, in: K-1 technical report, 1., edited by: Hasumi, H. and Emori, S., Center for climate system research, University of Tokyo, Japan, 34 pp., 2004. 3858

Kageyama, M., Laîné, A., Abe-Ouchi, A., Braconnot, P., Cortijo, E., Crucifix, M., de Vernal, A., Guiot, J., Hewitt, C. D., Kitoh, A., Kucera, M., Marti, O., Ohgaito, R., Otto-Bliesner, B., Peltier, W. R., Vettoretti, G., Weber, S. L., and MARGO project members: Last Glacial Maximum temperatures over the North Atlantic, Europe and Western Siberia: a comparison between PMIP models, MARGO sea-surface temperatures and pollen-based reconstructions, Quaternary Sci. Rev., 25, 2082–2102, 2006. 3842

Kageyama, M., Mignot, J., Swingedouw, D., Marzin, C., Alkama, R., and Marti, O.: Glacial climate sensitivity to different states of the Atlantic Meridional Overturning Circulation: results from the IPSL model, Clim. Past, 5, 551–570, doi:10.5194/cp-5-551-2009, 2009. 3837, 3843, 3859

Kageyama, M., Paul, A., Roche, D. M., and van Meerbeeck, C. J.: Modelling glacial climatic millennial-scale variability related to changes in the Atlantic meridional overturning circulation: a review, Quaternary Sci. Rev., 29, 2931–2956, 2010. 3835, 3837, 3850

Leuschner, D. C. and Sirocko, F.: The low-latitude monsoon climate during Dansgaard–Oeschger cycles and Heinrich Events, Quaternary Sci. Rev., 22, 925–941, 2000. 3836

Manabe, S. and Stouffer, R. J.: Two stable equilibria of a coupled ocean-atmosphere model, J. Climate, 1, 841–866, 1988. 3834

Marti, O., Braconnot, P., Dufresne, J.-L., Bellier, J., Benshila, R., Bony, S., Brockmann, P., Cadule, P., Caubel, A., Codron, F., de Noblet, N., Denvil, S., Fairhead, L., Fichefet, T., Foujols, M.-A., Friedlingstein, P., Goosse, H., Grandpeix, J.-Y., Guilyardi, E., Hourdin, F., Idelkadi, A., Kageyama, M., Krinner, G., Lévy, C., Madec, G., Mignot, J., Musat, I., Swingedouw, D., and Talandier, C.: Key features of the IPSL ocean atmosphere model and its sensitivity to atmospheric resolution, Clim. Dynam., 34, 1–26, doi:10.1007/s00382-009-0640-6, 2010. 3858

Marzin, C., Kallel, N., Kageyama, M., Duplessy, J.-C., and Braconnot, P.: Impact of rapid events on the Indian monsoon under glacial conditions: a model/data comparison study, Clim. Past Discuss., submitted, 2012. 3849

Merkel, U., Prange, M., and Schulz, M.: ENSO variability and teleconnections during glacial climates, Quaternary Sci. Rev., 29, 86–100, 2010. 3837, 3850, 3859

Mulitza, S., Prange, M., Stuut, J., Zabel, M., von Dobeneck, T., Itambi, A. C., Nizou, J., Schulz, M., and Wefer, G.: Sahel megadroughts triggered by glacial slowdowns of Atlantic meridional overturning, Paleoceanography, 23, PA4206, doi:10.1029/2008PA001637, 2008. 3836

Niedermeyer, E. M., Prange, M., Mulitza, S., Mollenhauer, G., Schefuss, E., and Schulz, M.: Extratropical forcing of Sahel aridity during Heinrich stadials, Geophys. Res. Lett., 36, L20707, doi:10.1029/2009GL039687, 2009. 3836, 3851

Otto-Bliesner, B. L. and Brady, E. C.: The sensitivity of the climate response to the magnitude and location of freshwater forcing: last glacial maximum experiments, Quaternary Sci. Rev., 29, 56–73, doi:10.1016/j.quascirev.2009.07.004, 2010. 3836, 3837, 3842, 3859

Otto-Bliesner, B. L., Hewitt, C. D., Marchitto, T. M., Brady, E., Abe-Ouchi, A., Crucifix, M., Murakami, S., and Weber, S. L.: Last Glacial Maximum ocean thermohaline circulation: PMIP2 model intercomparisons and data constraints, Geophys. Res. Lett., 34, L12706, doi:10.1029/2007GL029475, 2007. 3842

Pausata, F. S. R., Battisti, D. S., Nisancioglu, K. H., and Bitz, C. M.: Chinese stalagmite δ^{18}O controlled by changes in the Indian monsoon during a simulated Heinrich event, Nat. Geosci., 4, 474–480, 2011. 3850

Peterson, L. C., Haug, G. H., Hughen, K. A., and Röhl, U.: Rapid changes in the hydrologic cycle of the Tropical North Atlantic during the last glacial, Science, 290, 1947–1951, 2000. 3834, 3836

Pope, V., Gallani, M., Rowntree, P., and Stratton, R.: The impact of new physical parameterisations in the Hadley Centre climate model: HadAM3, Clim. Dynam., 16, 123–146, 2000. 3858

Prange, M., Romanova, V., and Lohmann, G.: The glacial thermohaline circulation: stable or unstable?, Geophys. Res. Lett., 29, 2028, doi:10.1029/2002GL015337, 2002. 3835

Roche, D., Paillard, D., and Cortijo, E.: Constraints on the duration and freshwater release of Heinrich event 4 through isotope modelling, Nature, 432, 379–382, 2004. 3839

Roche, D. M., Wiersma, A. P., and Renssen, H.: A systematic study of the impact of freshwater pulses with respoect to different geographical locations, Clim. Dynam., 34, 997–1013, 2010. 3836, 3837, 3859

Sánchez-Goñi, M.-F., Cacho, I., Turon, J.-L., Guiot, J., Sierro, F. J., Peypouquet, J.-P., Grimalt, J. O., and Shackleton, N. J.: Synchroneity between marine and terrestrial responses to millennial scale climatic variability during the last glacial period in the Mediterranean region, Clim. Dynam., 19, 95–105, 2002. 3836

Singarayer, J. S. and Valdes, P. J.: High-latitude climate sensitivity to ice-sheet forcing over the last 120 kyr, Quaternary Sci. Rev., 29, 43–55, 2010. 3837, 3859

Stocker, T. F. and Johnsen, S. J.: A minimum thermodynamic model for the bipolar seesaw, Paleoceanography, 18, 1087, doi:10.1029/2003PA000920, 2003. 3834

Stommel, H. M.: Thermohaline convection with two stable regimes of flow, Tellus, 13, 224–230, 1961. 3834

Stouffer, R. J., Yin, J., Gregory, J. M., Diwon, K. W., Spelman, M. J., Hurlin, W., Weaver, A. J., Eby, M., Flato, G. M., Hasumi, H., Hu, A., Jungclaus, J. H., Kamenovich, I. V., Levermann, A., Montoya, M., Murakami, S., Nawrath, S., Oka, A., Peltier, W. R., Robitaille, D. Y., Sokolov, A., Vettoretti, G., and Weber, S. L.: Investigating the causes of the response of the thermohaline circulation to past and future climate changes, J. Climate, 19, 1365–1387, 2006. 3834, 3835, 3838, 3841, 3849, 3850, 3851

Swingedouw, D., Braconnot, P., and Marti, O.: Sensitivity of the Atlantic Meridional Overturning Circulation to the melting from northern glaciers in climate change experiments, Geophys. Res. Lett., 33, L07711, doi:10.1029/2006GL025765, 2006. 3834

Swingedouw, D., Mignot, J., Braconnot, P., Mosquet, E., Kageyama, M., and Alkama, R.: Impact of freshwater release in the North Atlantic under different climate conditions in an OAGCM, J. Climate, 22, 6377–6403, 2009. 3837

Van Meerbeeck, C. J., Renssen, H., and Roche, D. M.: How did Marine Isotope Stage 3 and Last Glacial Maximum climates differ? – Perspectives from equilibrium simulations, Clim. Past, 5, 33–51, doi:10.5194/cp-5-33-2009, 2009. 3850

Voelker, A. H. L.: Global distribution of centennial-scale records for Marine Isotope Stage (MIS) 3: a database, Quaternary Sci. Rev., 21, 1185–1212, 2002. 3834

Wang, X., Auler, A. S., Edwards, R. L., Cheng, H., Cristalli, P. S., Smart, P. L., Richards, D. A., and Shen, C.-C.: Wet periods in Northeastern Brazil over the past 210 kyr linked to distant climate anomalies, Nature, 432, 740–743, 2004. 3834, 3836

Wang, Y. J., Cheng, H., Edwards, R. L., An, Z. S., Wu, J. Y., Shen, C.-C., and Dorale, J. A.: A high-resolution absolute-dated late Pleistocene monsoon record from Hulu Cave, China, Science, 294, 2345–2348, 2001. 3834, 3836

Wei, W. and Lohmann, G.: Simulated Atlantic Multidecadal Oscillation during the Holocene, J. Climate, doi:10.1175/JCLI-D-11-00667.1, in press, 2012. 3858

Yeager, S., Shields, C., Large, W., and Hack, J.: The low-resolution CCSM3, J. Climate, 19, 2545–2566, 2006. 3858

Zhang, X., Lohmann, G., Knorr, G., and Xu, X.: Two ocean states during the Last Glacial Maximum, Clim. Past Discuss., 8, 3015–3041, doi:10.5194/cpd-8-3015-2012, 2012. 3837, 3838, 3859

Table 1. Models compared in this analysis.

Experiment abbreviation	Model full name	Resolution	Reference
CCSM-NCAR	CCSM3	Atmosphere: T42L26 – Ocean 1°	Collins et al. (2006)
CCSM-MARUM	CCSM3	Atmosphere: T31L26 – Ocean 3°	Collins et al. (2006), Yeager et al. (2006)
MIROC1	MIROC	Atmosphere: T42L20 – Ocean 1.4°	K-1 model developers (2004)
MIROC2	as above		
IPSL	IPSL-CM4	Atmosphere: 96 × 72 × 19 – Ocean: 2°	Marti et al. (2010)
LCM10-0.15	LOVECLIM	Atmosphere:T21L3 – Ocean: 3°	Driesschaert et al. (2007)
LCM10-0.30	as above		
HadCM3-0.1	HadCM3	Atmosphere: 3.75° × 2.5° L19 – Ocean: 1.25°	Gordon et al. (2000), Pope et al. (2000)
HadCM3-0.4	as above		
COSMOS-S	COSMOS-aso	Atmosphere:T31L19 – Ocean 3° × 1.8°	Wei and Lohmann (2012)
COSMOS-W	see above		

CPD
8, 3831–3869, 2012

Table 2. Brief description of the experiments compared in this analysis.

Experiment abbreviation	Hosing experiment	Years taken for average	Reference for the hosing experiment
CCSM-NCAR	0.1 Sv for 500 yr in North Atlantic, 50–70° N	250–299	Otto-Bliesner and Brady (2010)
CCSM-MARUM	0.2 Sv in Greenland-Iceland-Norwegian Seas for 360 yr	last 100 yr for the AMOC, last 20 yr for the climate variables	Merkel et al. (2010)
MIROC1	0.1 Sv in North Atlantic (50–70° N) for 500 yr	370–419	
MIROC2	0.1 Sv in North Atlantic (50–70° N) for 500 yr	370–419	
IPSL	0.1 Sv in North Atlantic (50–70° N) for 419 yr	370–419	Kageyama et al. (2009)
LCM10-0.15	0.15 Sv in "Ruddiman Belt" (i.e. North Atlantic, 40–50° N)	350–400	Roche et al. (2010)
LCM10-0.30	0.30 Sv in "Ruddiman Belt"	220–240	Roche et al. (2010)
HadCM3-0.1	0.1 Sv in North Atlantic (50–70° N) for 1000 yr, reference experiment: 24 kyr BP	270–299	Singarayer and Valdes (2010) for similar 1 Sv hosing experiments and full description of reference experiment for 24 kyr BP
HadCM3-0.4	0.4 Sv in North Atlantic (50–70° N) for 1000 yr, reference experiment: 24 kyr BP	270–299	cf. above
COSMOS-S	0.2 Sv in North Atlantic Ruddiman Belt) for 150 yr, reference state: "strong" AMOC	years 140–150	Zhang et al. (2012)
COSMOS-W	0.2 Sv in North Atlantic Ruddiman Belt) for 250 yr, reference state: "weak" AMOC	years 200–250	

CPD
8, 3831–3869, 2012

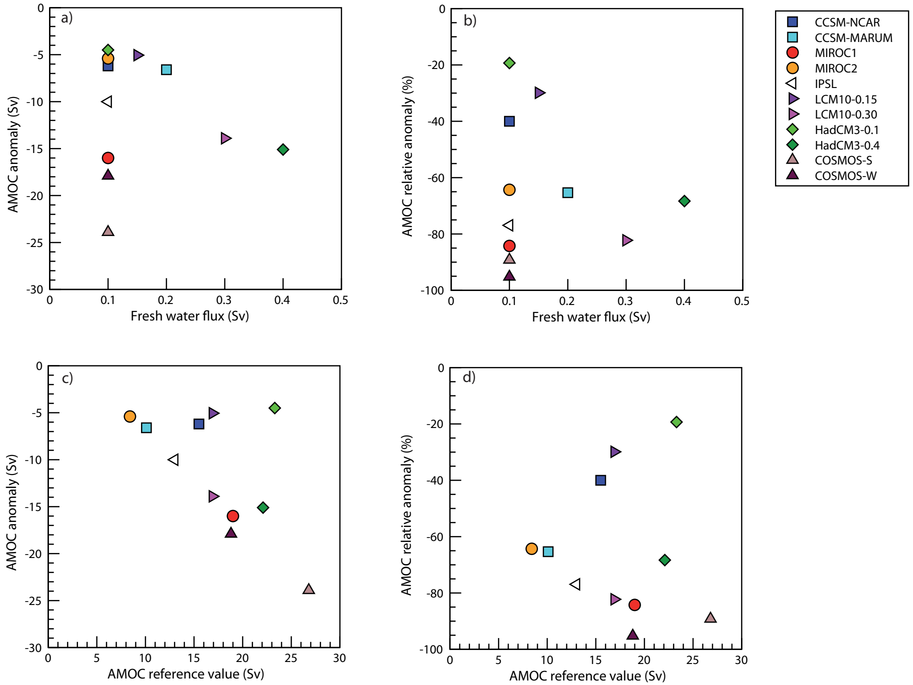

Fig. 1. Summary of AMOC behaviour in the different fresh water hosing simulations. The AMOC is defined as the mass export by the Atlantic Ocean at 30° S.

CPD
8, 3831–3869, 2012

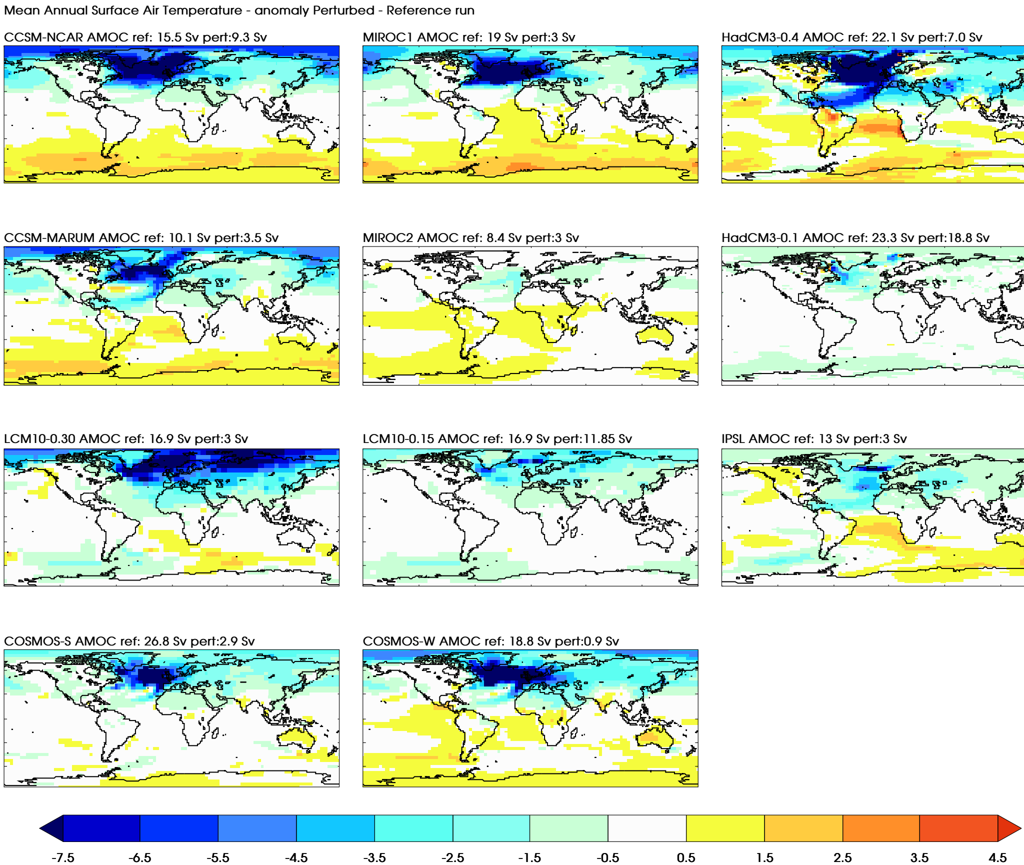

Fig. 2. Mean Annual Surface Air temperature response (hosing experiment – reference experiment, in K) to fresh water hosing for the 11 models.

CPD
8, 3831–3869, 2012

Climatic impacts of FW hosing for LGM conditions

M. Kageyama et al.

Title Page
Abstract Introduction
Conclusions References
Tables Figures
◀ ▶
Back Close
Full Screen / Esc
Printer-friendly Version
Interactive Discussion

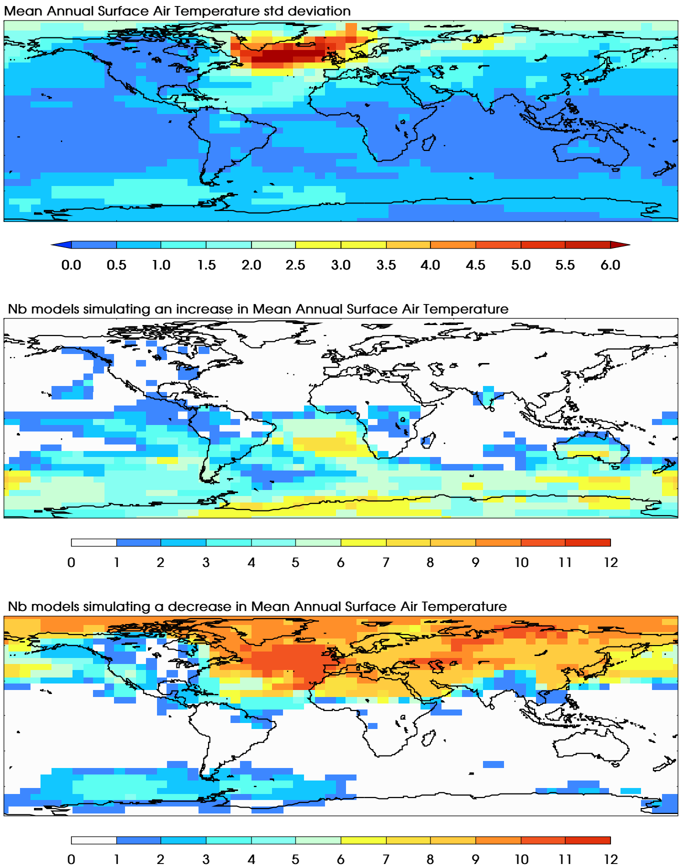

Fig. 3. (Top) Standard deviation of the mean annual temperature response across the 11 models (in K); (middle) number of models showing an increase larger than 0.5 K between the perturbed and the reference experiments; (bottom) number of models showing a decrease larger than 0.5 K (in amplitude) between the perturbed and the reference experiments.

CPD
8, 3831–3869, 2012

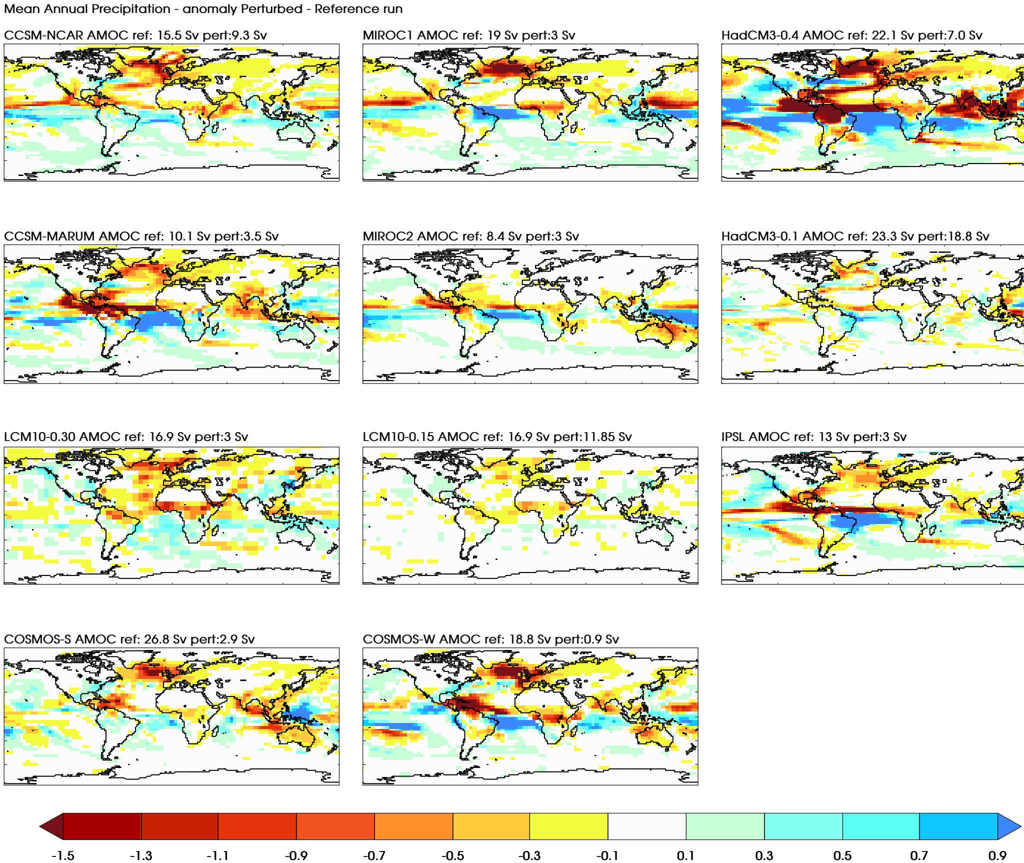

Fig. 4. Mean Annual Precipitation response (hosing experiment – reference experiment, in mm day^{-1}) to fresh water hosing for the 11 models.

CPD
8, 3831–3869, 2012

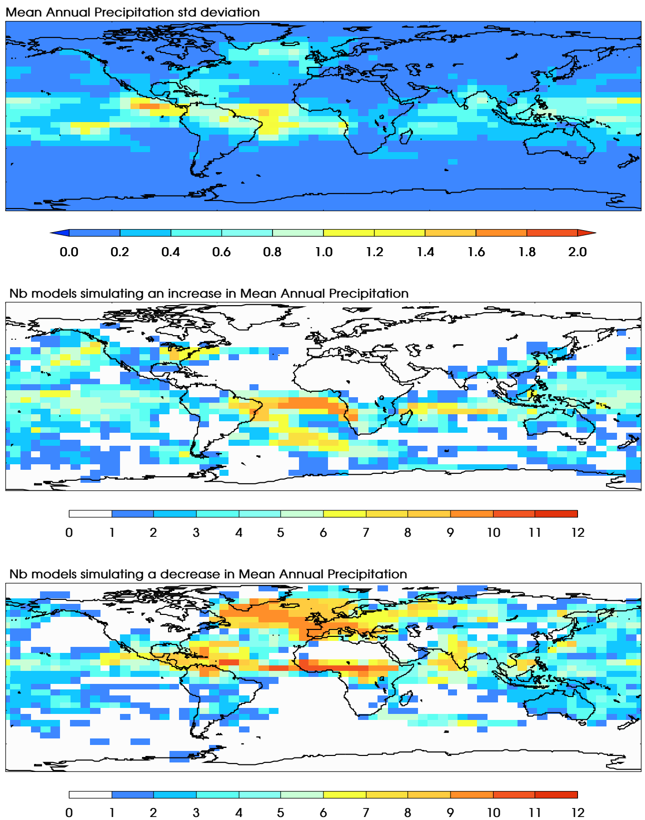

Fig. 5. (Top) Standard deviation of the mean annual precipitation response across the 11 models (in mm day^{-1}); (middle) number of models showing an increase larger than 0.1 mm day^{-1} between the perturbed and the reference experiments; (bottom) number of models showing a decrease larger than 0.1 mm day^{-1} (in amplitude) between the perturbed and the reference experiments.

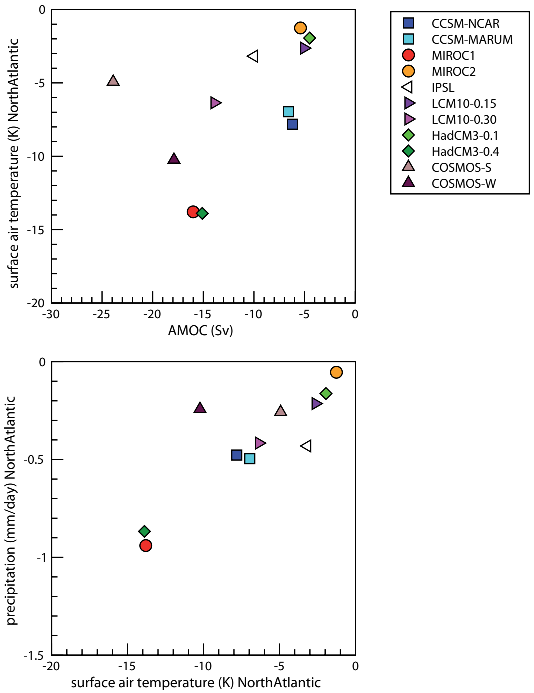

Fig. 6. Relationships for the North Atlantic extratropics, (top) between the changes (related to hosing) in mean annual surface air temperature averaged over this region and the AMOC changes and (bottom) between the changes in mean annual temperatures and mean annual precipitation averaged over this region. This region is defined for longitudes between 50 and 10° W and latitudes between 40 and 60° N.

CPD
8, 3831–3869, 2012

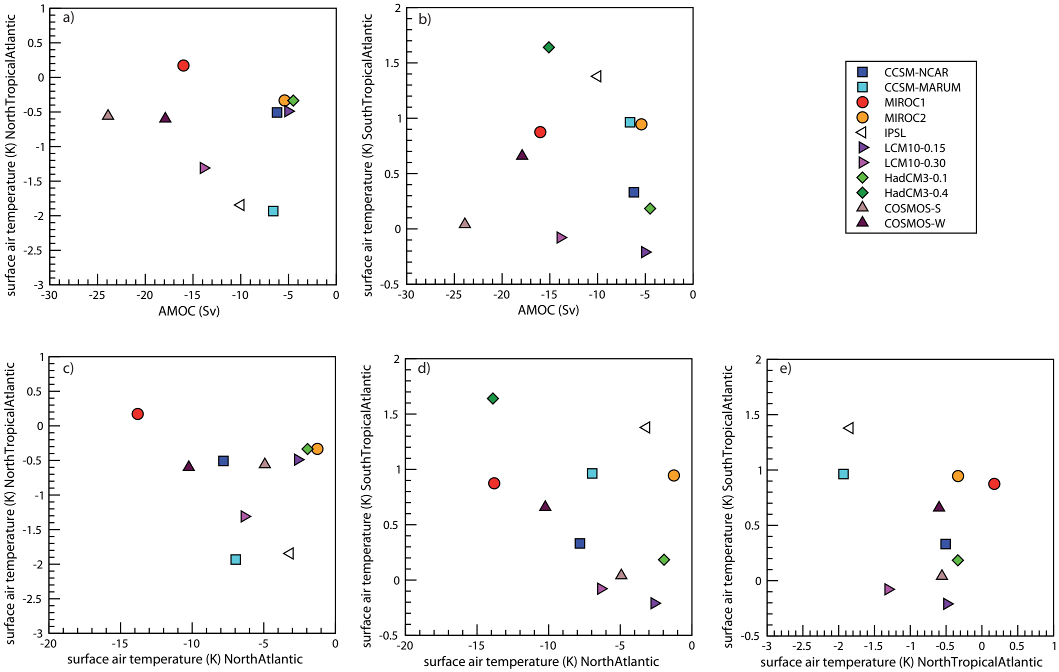

Fig. 7. Relationships involving tropical Atlantic temperatures changes related to fresh water hosing. The "NorthTropicalAtlantic" region is defined as the region with latitudes included between 5 and 30° N and longitudes between 50 and 15° W. The "SouthTropicalAtlantic" region is defined as the region with latitudes included between 20° S and 5° N and longitudes between 30° W and 10° E. Top: relationships between temperature changes over these regions and AMOC changes. Bottom: (left and middle) relationships between temperature changes over these regions and the North Atlantic (region defined in Fig. 6) temperature changes; (right) relationship between the temperature changes over the North and South Tropical Atlantic regions.

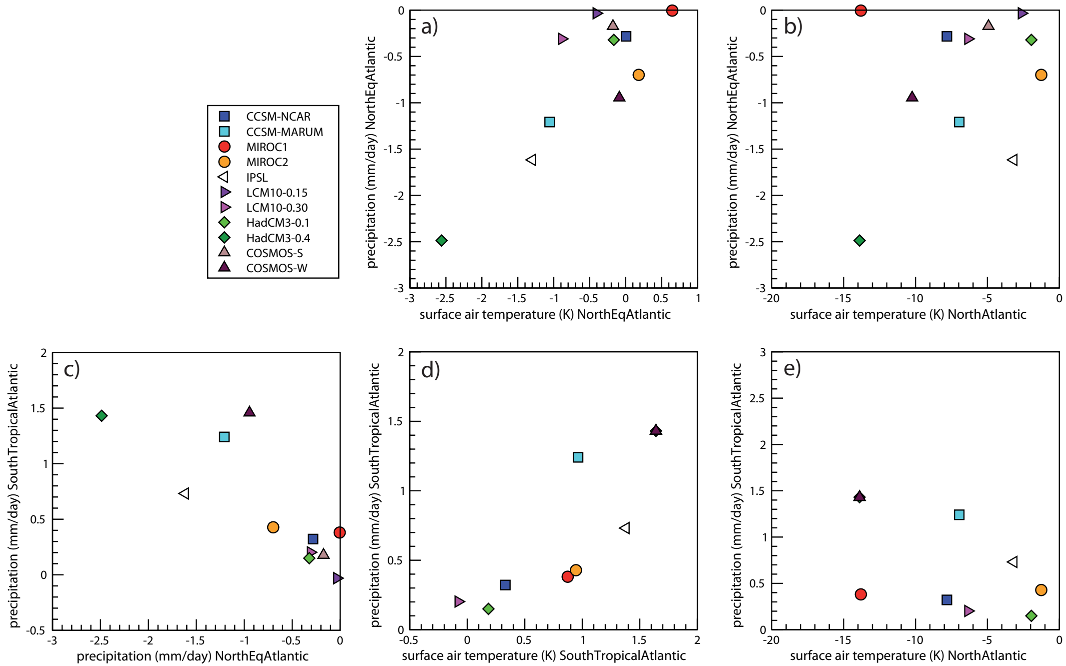

Fig. 8. Relationships involving tropical Atlantic precipitation changes related to fresh water hosing: **(a)** between the precipitation and temperature changes over the NorthEqAtlantic region, defined as the region with latitudes ranging between 5 and 15° N; **(b)** between the NorthEqAtlantic precipitation changes and the NorthAtlantic (as defined in Fig. 6) temperature changes, **(c)** between the precipitation changes over the SouthTropicalAtlantic and the NorthEqAtlantic region, **(d)** between the precipitation and temperature changes over the SouthTropicalAtlantic region defined as in Fig. 7, **(e)** between the SouthTropicalAtlantic precipitation changes and the NorthAtlantic emperature changes.

CPD
8, 3831–3869, 2012

Climatic impacts of FW hosing for LGM conditions

M. Kageyama et al.

Title Page
Abstract Introduction
Conclusions References
Tables Figures
◂ ▸
Back Close
Full Screen / Esc
Printer-friendly Version
Interactive Discussion

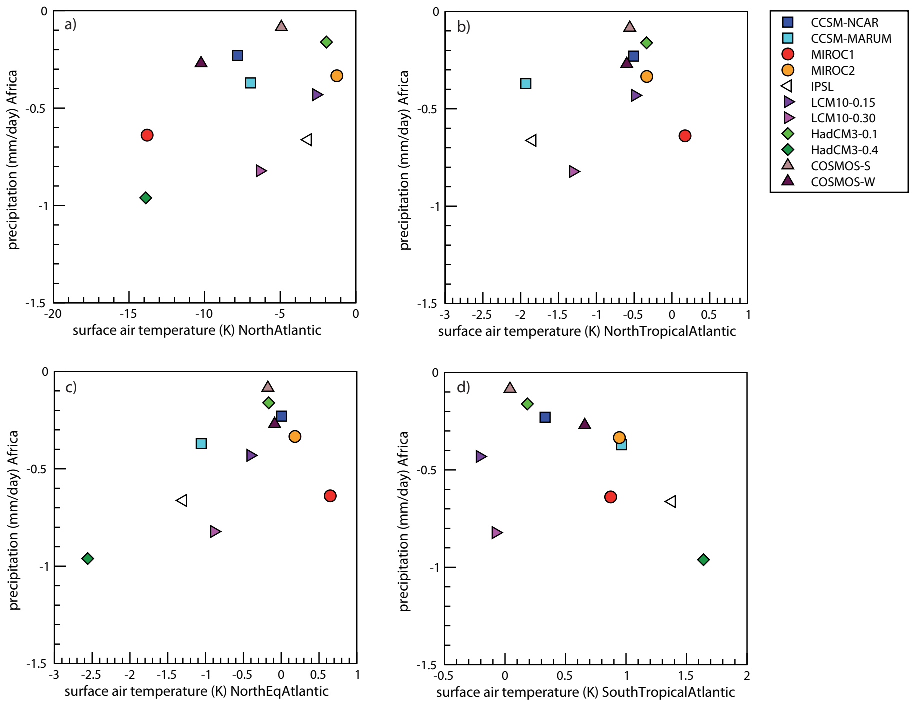

Fig. 9. Relationships involving precipitation changes over the African monsoon region, defined for latitudes between 5 and 15° N and longitudes between 15° W and 15° E.

CPD
8, 3831–3869, 2012

Title Page
Abstract Introduction
Conclusions References
Tables Figures
◀ ▶
Back Close
Full Screen / Esc
Printer-friendly Version
Interactive Discussion

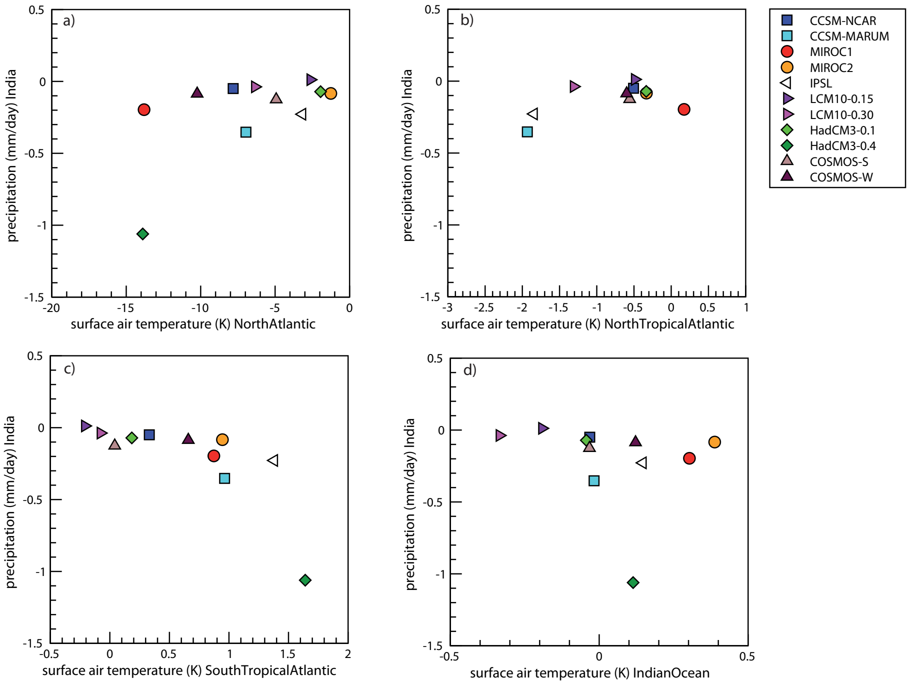

Fig. 10. Relationship involving precipitation changes over the Indian monsoon region, defined for latitudes ranging between 10 and 30° N and longitudes between 60 and 90° E. The Indian Ocean region is defined for latitudes ranging between 10° S and 15° N and longitudes between 50 and 1O0° E. The "NorthTropicalAtlantic" and "SouthTropicalAtlantic" regions are the same as defined in Fig. 7.

CPD
8, 3831–3869, 2012

Climatic impacts of FW hosing for LGM conditions

M. Kageyama et al.